optica

High-sensitivity optical-fiber-compatible photodetector with an integrated $CsPbBr_3$-graphene hybrid structure

JIN-HUI CHEN[1], QIANG JING[1], FEI XU[1,*], ZHEN-DA LU[1,2] & YAN-QING LU[1]

[1]National Laboratory of Solid State Microstructures, College of Engineering and Applied Sciences and Collaborative Innovation Center of Advanced Microstructures, Nanjing University, Nanjing 210093, China
[2]e-mail: luzhenda@nju.edu.cn
[3]e-mail: yqlu@nju.edu.cn
*Corresponding author: feixu@nju.edu.cn

Published 21 July 2017

This document provides supplementary information to "High-sensitivity optical-fiber-compatible photodetector with an integrated CsPbBr3-graphene hybrid structure," https://doi.org/10.1364/optica.4.000835. Four figures and one table are provided, which include experimental results and performance comparisons of devices. More fabrication process details and measurements are also provided.

https://doi.org/10.6084/m9.figshare.5187604

Supplementary Note 1: The fabrication process of devices and characterizations.

Materials. Cs_2CO_3, octadecene, oleic acid, $PbBr_2$, oleylamine were all purchased from Aladdin and used as received without further purification. The multilayered graphene on copper foil are purchased from Six Carbon Technology (Shenzhen, China).

Synthesis of $CsPbBr_3$ NCs. Cs_2CO_3 (0.407 g) was loaded into a 50 mL three-neck flask along with octadecene (20 mL) and oleic acid (1.25 mL). The mixture was then degassed for 0.5 h at 120°C, and heated to 150°C under N_2 atmosphere to form a clear solution. Octadecene (5mL) and $PbBr_2$ (0.1 g) were loaded into 50 mL three-neck flask along with oleylamine (1 mL) and oleic acid (0.5 mL). The mixture was degassed for 0.5 h at 120°C. After complete solubilisation of the $PbBr_2$ salt, the temperature was raised to 150℃, and Cs-oleate solution (0.5 mL, prepared as described above) was quickly injected. After 5 s, the reaction mixture was cooled down by an ice-water bath. After cooling down to room temperature, ethanol or acetone was added to the solution to precipitate perovskite nanoparticles, which were then separated by centrifugation. Finally, the resulting nanoparticles were re-dispersed into 5 mL cyclohexane.

Nanomaterials and device characterization. TEM and high-resolution TEM were performed on a FEI Tecnai G2 F20 electron microscope operating at 200 kV. X-ray powder diffraction measurements were done using a Bruker AXS D8 X-ray diffractometer equipped with monochromatized Cu Kα radiation (λ=1.5418Å). Ultraviolet and visible absorption spectra were recorded with a Beituo DUV-18S2 and a Shimadzu UV-3600 plus spectrophotometer at room temperature. PL excitation and emission spectra were measured with a Hitachi F4500 fluorescence spectrophotometer, a home-made fiber fluorimeter system and a compact spectrometer purchased from Thorlabs. The in-situ transmission spectrum of FCPD was collected by 20× object lens (NIKON) and analyzed by high sensitive spectrometer (NOVA, ideaoptics, China). Raman spectroscopy were performed at room temperature in air with LabRam HR 800 Evolution system (HORIBA Jobin Yvon) with an excitation line of 532 nm. The Raman band of the Si at 520 cm^{-1} was used as a reference to calibrate the spectrometer.

Device fabrication. First, a single-mode fiber protective coating was peeled off and was washed in ethanol with ultrasonic for a few minutes. Second, the fiber's end surface was cleaved (CT-38, Fujikura) and a flat platform on the facet was created. Third, the fiber was placed in a film deposition equipment (K550X, EMTTECH) under vacuum (5×10^{-2} mbar) at a deposition speed of ~7.5 nm/min for 4 min. The gold film on the facet was scratched into a narrow channel using a tapered tungsten probe under an optical microscope, while the lateral electrodes were directly obtained by using a lapping film (LF1P, Thorlabs). The typical channel is 9 μm in length and 125 μm in width. Fourth, the graphene on the copper foil was etched with 2M $FeCl_3$ solution and washed with deionized water several times. The graphene was transferred to a prepared optical fiber's end surface (described above) using a dip-coating method. A cleaved optical fiber with pair gold electrodes was moved down slowly toward the floating graphene until it touched the graphene sample. And the graphene was attached to the fiber substrate. The sample was then annealed at 200 °C in air for an hour. Fifth, the prepared $CsPbBr_3$ cyclohexane solution was directly dropped casting onto graphene (on fiber) and washed with isopropanol for a minute to remove ligands on $CsPbBr_3$ NCs. We can find that the graphene transfer process is in no need of a layer of conventional polymer like poly (methyl methacrylate) (PMMA). As a result, this kind of transfer technique is not suitable for monolayer graphene, which is very fragile in transferring process. In our lab, we find that

multilayer graphene rather than monolayer is best fit for the dip-coating process.

Photoelectrical characterization. We designed a parallel metal plate to connect the fiber electrodes and exert bias voltage on the FCPD. The photoelectrical characterizations were based on a sourcemeter (Keithley 2400) controlled by Labview programs. The devices were illuminated by monochromatic light from a light-emitting diode (400 nm or 532 nm) and filtered supercontinuum light source (NKT Photonics, K91-120-02). The long term stability experiment was conducted continuously for an hour every 24 hours over a week. All the experiments were conducted in ambient environment.

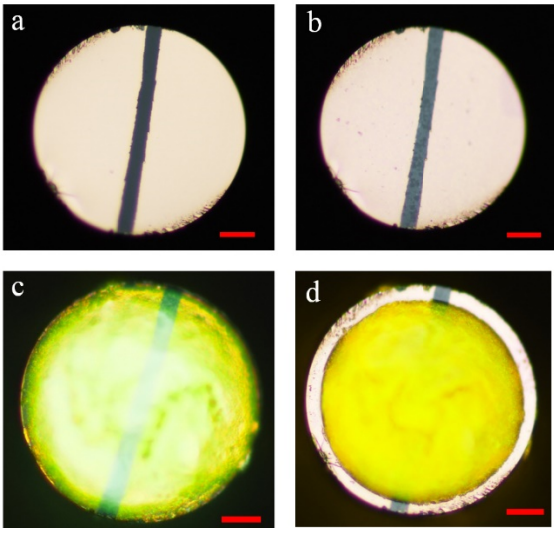

Fig. S1. The sequential fabrication process of FCPD. (a) An optical fiber deposited with two separated gold electrodes. (b) After depositing a multilayered graphene. (c) After drop-casting $CsPbBr_3$ NCs cyclohexane solution. (d) After washed with isopropanol for 60 seconds. The scale bar is 20 μm.

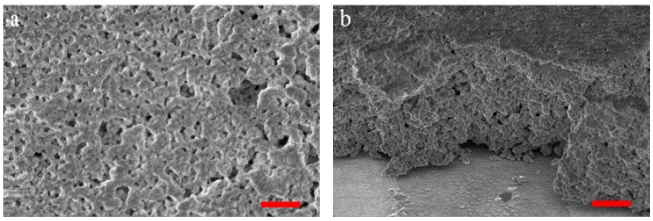

Fig. S2. The scanning electron microscopy (SEM) image of self-assemble $CsPbBr_3$ NCs film. The scale bar is 500 nm (a) and 2 μm (b).

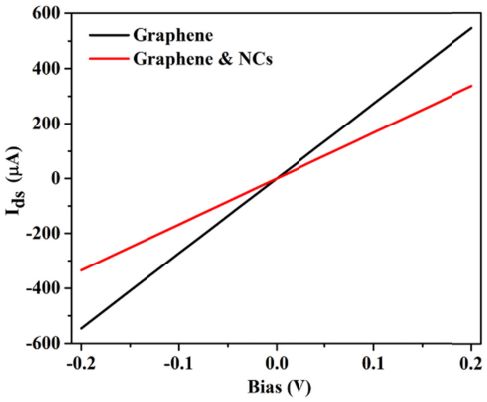

Fig. S3. The measured I-V curve for graphene only devices and graphene-$CsPbBr_3$ hybrid devices.

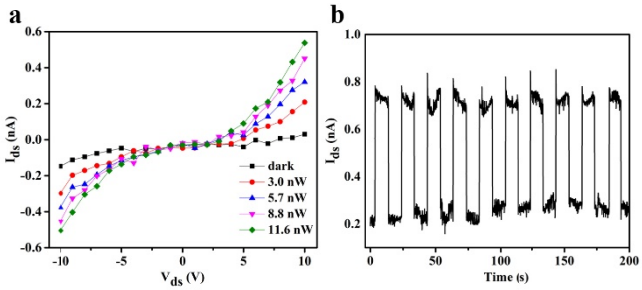

Fig. S4. The photoresponse for $CsPbBr_3$ only FCPD device. (a) The *I-V* curve in darkness and with light illumination (@ 400 nm). (b) The dynamical response of device at 10 V bias with 11.5 nW light illumination (@ 400 nm).

Supplementary Note 2: Numerical fitting model for transmission spectrum of multilayered graphene

Since multilayered graphene is only of a few nanometers thickness, we treat graphene as a boundary condition in the numerical model. By solve the Maxwell equation, a modified Fresnel equation is derived:

$$T = \frac{4 n_{SiO_2} n_{Air}}{(n_{SiO_2} + n_{SiO_2} + \sqrt{\mu_0 / \varepsilon_0} N\sigma)^2}$$

where μ_0, ε_0, N and σ are vacuum permeability, vacuum permittivity, graphene layer numbers and graphene conductivity [1]. Taking the transmission formula without graphene as reference, the transmission T' should be:

$$T' = \frac{1}{(1 + \sqrt{\mu_0 / \varepsilon_0} N\sigma / (n_{SiO_2} + n_{Air}))^2}$$

Table S1. Figures-of –merit for graphene and all-inorganic perovskites based photodetectors

		Measurement conditions				Device performance		
Materials	Platform	V_{ds} (V)	V_g (V)	λ (nm)	P (mW/cm^2)	Responsivity (A/W)	Rise time (s)	Ref.
Bilayer graphene & $CsPbBr_{3-x}I_x$	Si/SiO_2	1	-60	405	7×10^{-5}	8.2×10^{8}	0.81	[2]
Monolayer graphene & $MAPbI_3$	Si/SiO_2	0.1	-	520	2	1.8×10^{2}	0.087	[3]
Graphene & $MAPbBr_2I$ island*	Si/SiO_2	3	0	405	1.02 nW	6.0×10^{5}	0.12	[4]
Graphene & $MAPbI_{3-x}Cl_x$	Si/SiO_2	0.1	-25	598	1.42×10^{-5}	1.8×10^{8}	-	[5]
Monolayer graphene & $MAPbI_3$	Polyimide (flexible)	1	0	515	-	1.15×10^{2}	0.25	[6]
Multilayered graphene & $CsPbBr_3$	SiO_2 (optical fiber)	0.2	0	400	7.5×10^{-2}	2×10^{4}	3.1	**This work**

* Interdigital electrode

We can find that all the devices show high responsivity while quite slow response speed. It is because there are trap states in all these devices. The trap states can enhance the responsivity of devices (photogain) at the cost of response speed. And the trap states are mainly determined by the materials quality and the interfacial properties. It is known that the solution processed nanocrystals/quantum dots have surface ligands and defects, which contributing to the trap states. And these defects can be repaired by surface passivation or ligand exchange techniques [7]. We figure that the different response time might be attributed to the different materials quality, fabrication technology and the device configurations.

References

1. Z. Chen, J. Chen, Z. Wu, W. Hu, X. Zhang, and Y. Lu, Appl. Phys. Lett. **104**, 161114 (2014).
2. D. H. Kwak, D. H. Lim, H. S. Ra, P. Ramasamy, and J. S. Lee, RSC Adv. **6**, 65252 (2016).
3. Y. Lee, J. Kwon, E. Hwang, C. H. Ra, W. J. Yoo, J. H. Ahn, J. H. Park, and J. H. Cho, Adv. Mater. **27**, 41 (2015).
4. Y. Wang, Y. Zhang, Y. Lu, W. Xu, H. Mu, C. Chen, H. Qiao, J. Song, S. Li, and B. Sun, Adv. Opt. Mater. **3**, 1389 (2015).
5. C. Xie, and F. Yan, ACS Appl. Mater. Interfaces, **9**, 1569 (2017).
6. V. Q. Dang, G. S. Han, T. Q. Trung, T. D. Le, Y. U. Jin, B. U. Hwang, H. S. Jung, and N. E. Lee, Carbon **105**, 353 (2016).
7. G. Konstantatos, I. Howard, A. Fischer, S. Hoogland, J. Clifford, E. Klem, L. Levina, and E. H. Sargent, Nature, **442**, 180, 2006.